Int. J. Electrochem. Sci., 17**(2022)** Article Number: 221298, doi: 10.20964/2022.12.101

International Journal of ELECTROCHEMICAL SCIENCE
www.electrochemsci.org

Short Communication

Effect of Chloride on Accelerated Corrosion of Steel Rebar in Alkali-Activated Fly Ash and Paper Sludge Ash–Reinforced Concrete

P. Senthamilselvi[1,*], *T. Palanisamy*[2] *and S.Senthilkumar*[3]

[1] Department of Civil Engineering, Government College of Engineering, Salem 636011, Tamil Nadu, India
[2] Department of Civil Engineering, National Institute of Technology, Suratkal 575025,Karnataka, India
[3] Department of Civil Engineering, KSR College of Engineering, Tiruchengode 637215, Tamil Nadu, India
[*]E-mail: senitaarul2009@gmail.com

Received: 15 July 2022/ *Accepted:* 23 November 2022 / *Published:* 27 December 2022

The aim of this work was to investigate the corrosion of reinforcing rebar inserted in geopolymer concrete (GPC) made from fly ash (FA) containing 10% paper sludge ash (PSA) by weight under three curing conditions, namely oven curing (OC) at 60°C, external exposure curing(EEC), and curing at ambient temperature (AC). The investigation was carried out on the GPC using linear polarization resistance and Tafel plot techniques. All of the reinforced lollipop specimens were stored in a 3.5% NaCl solution with a steady anodic electrical potential of about 12 V applied to accelerate the corrosion process. Both the bond strength loss percentage and the mass loss percentage of the corroded steel rebar embedded in the concrete cylinder specimens were calculated. The test results showed that the OC condition demonstrated best corrosion resistance in the FA-GPC specimen compared to the FA-PSA GPC specimen. The test results for FA-PSA GPC specimens showed that their corrosion resistance performance was better under AC condition compared to the other two curing conditions.

Keywords: Geopolymers; fly ash; corrosion; curing; paper sludge ash

1. INTRODUCTION

The amount of cement produced globally has been constantly increasing. It reached3.6 billion tonnes in 2011[1].It is known that Portland cement production requires considerable energy and releases carbon dioxide (CO_2) into the atmosphere by calcination process of limestone and from the combustion of fossil fuels during the process. One tonne of CO_2 is released into the environment from the manufacturing of 1tonne of cement [2]. Hence, there is an urgent need to further develop

cementitious products with decreased environmental impacts and greater economic benefits. Production of geopolymer concrete (GPC), which has emerged as an alternative construction material that completely replaces the cement in the mixture, has been described as one of the most revolutionary developments in concrete construction. With metakaolin (MK) and slag as the source materials, fly ash (FA) has now been transformed as a primary component of the geopolymer. GPC with a strength of up to 55 MPa can also be produced using FA and the effluent alkaline solution from poly-fiber factories [3].

The final product, known as aluminosilicates, was formed by a chemical reaction between silica and alumina present in FA and alkaline solutions during the synthesis of FA geopolymer, which requires activating reactive silica and alumina in the FA[4].

According to some reports, low-calcium FA-based GPC has greater corrosion resistance in the marine environment compared to ordinary Portland cement (OPC) due to its resistance to chloride penetration [5]. It was discovered that the propagation stage of the corrosion process in FA-GPC was comparable to that occurring in Portland cement concrete [6].Depending on the type of activation and external factors it is subjected to, steel reinforcement in alkali-activated FA mortars will passivate [7].

According to several investigations, FA-GPC exhibits improved corrosion resistance when sodium silicate and sodium hydroxide concentrations are increased[8].Patil and Allouche [9] concluded that the class F FA-based GPC shows a lower chloride diffusion coefficient, porosity, and chloride content in comparison to class C FA-GPC and OPC specimens by showing higher resistance to chloride-induced corrosion. In a study conducted by Olivia and Nikraz [10], the authors concluded that the presence of alkalinity in the GPC's pore solution would slow down the process of the reinforcement depassivation by chloride ions. The corrosion performance of a steel bar with the protective coating of MK-based GP showed a higher resistance to the corrosion process compared to that with a protective coating of FA-GP when exposed to chloride environment [11]. The same performance was also observed with MK-GP coating over the steel bar [12].

The chloride diffusion coefficient of bi-blended GPCs with FA and slag as source material is lower than that of OPC concrete, whose diffusion coefficient falls with increasing slag concentration in the binder. [13].Another investigation comparing FA-GPC with kaolin-based GPC showed that the best corrosion performance was achieved by passivating the steel reinforcement by kaolin-based GPC in both the aggressive media of distilled water and ASTM seawater, whereas FA-GPC showed better passivation only under distilled water and not in ASTM seawater [14].

Paper sludge ash (PSA) is another pozzolanic substance that has not been widely used in the geopolymer field. Very few studies have been conducted on the characteristics of geopolymer mortar or concrete produced using waste PSA-based geopolymer binder [15–18].

Paper sludge, the main byproduct of the pulp and paper industry, is burned, producing PSA, which is a significant solid waste issue for the sector [19,20]. On incineration, the sludge can be transformed into a pozzolanic product,which can be used in the cement and concrete industries[16,21,22]. About 70%–80% of the PSA is made up of by amorphous silica and alumina[23].

This is a comparative study on the corrosion behavior of FA-GPC and FA-PSA GPC with 10% PSA, which were cured under various circumstances using linear polarization resistance (LPR) and Tafel plot (TP) techniques. The impressed voltage of approximately 12 V was used to charge the steel

bar in GPC to accelerate the corrosion test. Sodium chloride with approximately 3.5% concentration was used as an electrolyte. Polarization resistance, corrosion potential, current density, and corrosion rate (CR) were investigated using LPR and TP techniques. Bond strength loss of the steel bar in GPC and its mass loss were also determined to validate the experimental results.

This article reports the experimental data from the test results by comparing corrosion resistance in FA-GPC to FA-PSA GPC under three curing conditions, namely oven curing at 60°C (OC), external exposure curing (EEC), and curing at ambient temperature (AC).

2. MATERIALS AND SPECIMEN PREPARATION

In the manufacture of the GPC, FA, PSA, fine aggregate (river sand), coarse aggregate with a maximum size of 20 mm, alkaline sodium hydroxide (12 M) liquids, and sodium silicate solution were all used. Table 1 lists the mix proportions of FA-GPC and FA-PSA-based GPC. Table 2 shows the mechanical and chemical characteristics of the steel reinforcement used.

Mettur Thermal Power Station (Tamil Nadu, India) provided Class F FA for the study. The FA had a specific gravity of 2.29. Its bulk density was around 748 kg/m^3 for loose bulk and roughly 1077.3kg/m^3 for compacted bulk. Table 3 shows information about FA's chemical composition. Figures 1(a) and (b) show images of the FA obtained by scanning electron microscopy (SEM) and energy-dispersive X-ray spectroscopy (EDAX), respectively. The SEM image shows spherical FA particles with different sizes.

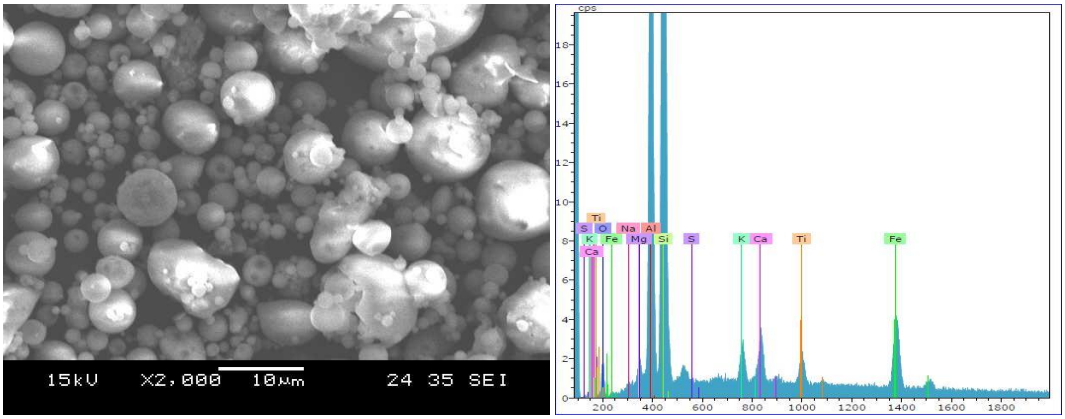

(a) (b)

Figure 1. (a) SEM image of fly ash and (b) EDAX image of fly ash.

Paper sludge from the Seshasayee Paper Mill (Pallipalayam, Erode, Tamil Nadu, India) was burned for 2h at 700°C to produce PSA. The PSA had a specific gravity of 2.3. It had a loose bulk density of around 384.3 kg/m^3 and compacted density of about 646.9 kg/m^3. The PSA was less bulky than the FA.. Table 3 shows chemical characteristics of the PSA. Figures 2(a) and (b) show, respectively,SEM and EDAX images of the PSA. As shown in the figure, the PSA particles are primarily hexagonal and platy.

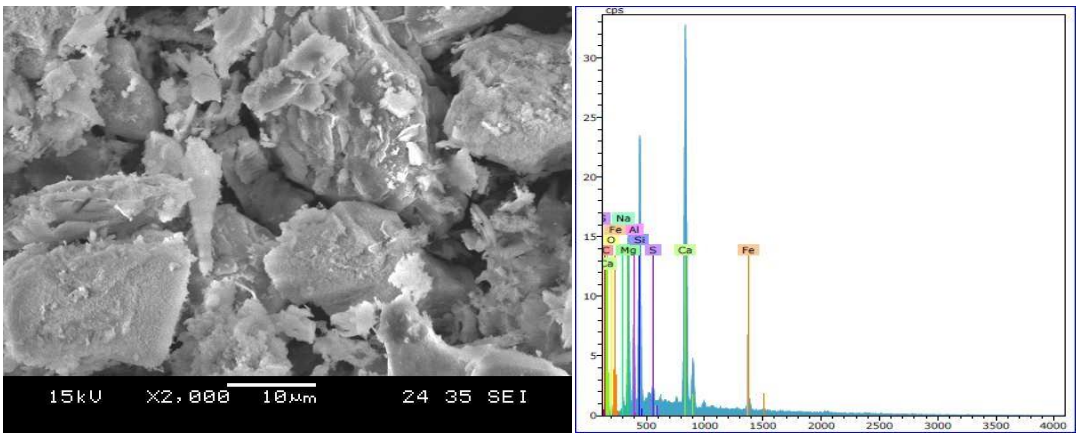

(a) (b)

Figure 2. (a) SEM image of paper sludge ash and (b) EDAX image of paper sludge ash.

In this study, two mixes Mix 1 and Mix 2 containing 100% FA-GPC mix and 90% FA–10% PSA-GPC mix respectively were considered. One 12-mm-diameter high-yield-strength deformed steel reinforcement bar was implanted in the concrete with a length of approximately100 mm to create lollipop-shaped GPC specimens with a characteristic strength of 35 MPa, which complied with IS 456. The exposed rebar outside the concrete was coated with epoxy to inhibit the external corrosion. To ensure a radial chloride attack, the epoxy was coated on the top and bottom sides of the cylindrical samples.To fix the mounting electrical connection to the sample, a screw thread system was adapted at the end parts of the bars.

Three curing regimes described earlier were used to observe the effect of inclusion of PSA on the corrosion behavior of FA-GPC.

Table 1. GPC mix proportions.

Material	**Mix 1 (kg/m^3)**	**Mix 2 (kg/m^3)**
	FA-GPC	**FA-PSA-GPC**
Fly ash	425.73	383.16
PSA	0	42.57
Coarse aggregate	1212.60	1212.60
Fine aggregate	642.50	642.50
NaOH solution	54.74	54.74
Na_2SiO_3 solution	136.84	136.84
Activator modulus	3.29	3.29

Table 2. Mechanical and chemicalproperties of reinforcement bar.

Type	**Mechanical Properties**	**Yield Capacity (MPa)**	**Tensile Capacity (MPa)**	**Modulus of Elasticity (GPa)**
Grade 500		560	660	206
	Chemical properties	**Carbon (%)**	**Sulfur (%)**	**Phosphorus (%)**
		0.3	0.55	0.55

Table 3 Mass percentage of chemical composition of the fly ash and paper sludge ash

Composition	**Fly ash (%)**	**Paper sludge ash (%)**
Silicon dioxide	53.97	35.25
Aluminum oxide	34.66	7.09
Ferrous oxide	5.3	2.83
Calcium oxide	1.96	37.42
Magnesium oxide	1.28	14.39
Sodium oxide	0.13	0.81
Sulfur oxide	0.25	0.69
Potassium oxide	0.93	0.85
Titanium oxide	1.52	0.67
LOI	2.6	0.63

2.1. Curing

The concrete samples were placed in the AC in a shaded location with a 28°C maximum temperature. Until the corrosion process started, these specimens were kept out of the sun and the rain all the time. The concrete samples in the EEC were set up in a location that was shielded from rain and received direct sunlight. The externally exposed method's highest temperature was 41°C. The specimens were also exposed to OC under 60°C exposure conditions for the sake of comparison. Before being put into an oven, the freshly cast specimens were given a 1-day wait. Following demolding, the samples were kept in an electrical oven set to 60°C for 24 h. The specimens were moved to ambient condition after the predetermined amount of time.

Labels A, B, and C, which stand for oven at 60 °C, external exposure, and ambient conditions, respectively, were used to identify different mixes. The numbers 0 and 10 were added to each alphabet to indicate the percentage of FA replaced by PSA, i.e., 100% FA-based GPC and 90% FA- and 10% PSA-based GPC, respectively.

This investigation was done to see how chloride-induced corrosion would affect reinforced GPC specimens made of class F FA and PSA.

As per the code IS 516-1959, the mechanical property, i.e., compressive strength, was tested using 150 × 150 × 150 mm mold.

2.2. Accelerated reinforced corrosion

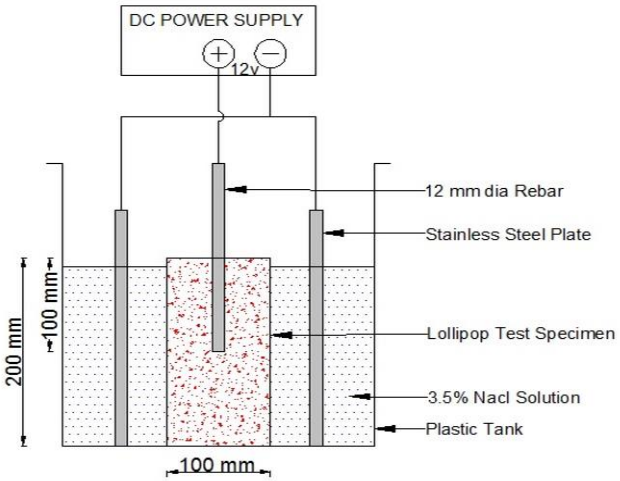

Figure 3. Illustration of the setup for an accelerated corrosion test.

To ensure complete saturation, the reinforced specimens were submerged in a 3.5% NaCl solution for 24 h.The solution was filled up in the tank up to the top of concrete surface. An anodic potential of 12 V was applied to start the corrosion process, and it was kept at that level for the whole 20-day corrosion period.This is an expedited electrochemical laboratory approach for investigating corrosion.It was created initially by the Nordtest [24] approach, then by the Florida Department of Transportation [25] and Sahmaran et al. [26].As shown in Figure 3, the procedure involves placing a stainless steel plate around the specimens, connecting it to the negative terminal of the power supply, and connecting the positive terminal to the reinforcing bar, which serves as the anode.

2.3. Corrosion monitoring

In this study, experiments using LPR and TP techniques were performed using a GILL AC potentiostat. A three-electrode arrangement was used to conduct the electrochemical test. It included a saturated calomel electrode as the working electrode, stainless steel as the counter electrode, and reinforcing steel as the reference electrode, as shown in Figure 4.

The LPR measurements were made between -50mV and +50 mV at a scan rate of 60 mV/min.According to Stern and Geary's [27] Equation (1), the LPR approach can be used to determine the rate of corrosion, which is described as follows:

$$I_{corr}=\beta_a\beta_c/2.3R_p\ (\beta_a+\beta_c) =B/R_p \quad (1)$$

where β_a and β_c are, respectively, the anodic and cathodic Tafel constants. R_p is the polarization resistance.This was determined by the potential–current density curve's slope at the zero current point[28].

$$R_p = (\Delta E/\Delta I)_{\Delta E\rightarrow 0} \quad (2)$$

where ΔI represents the current density and ΔE represents the applied potential.

The following formula was used to determine the CRs after the corrosion current density was determined:

$$CR = I_{corr} \times a/n \times F \quad (3)$$

Where a is the atomic weight, n is the number of equivalent exchanges, and F is the Faraday constant (96,500 coulombs/equivalent).

After the completion of electrochemical measurements, the pull-out test was conducted. Direct tension force was used to conduct the test on GPC cylindrical specimens.It was conducted on a universal testing machine (UTM) with a capacity of 1000 kN.Bond strength was calculated using the following formula:

$$\text{Bond strength} = P/A \quad (4)$$

where P is the maximum load and A is the total surface area of the rod in contact with the concrete.

At the end of the pull-out test, the destructive test was conducted. The concrete specimens were broken out and steel bars were extracted from concrete and cleaned off as per ASTM Standard G1 [29] to determine the mass loss of rebars by conducting gravimetric test to validate the electrochemical test results.

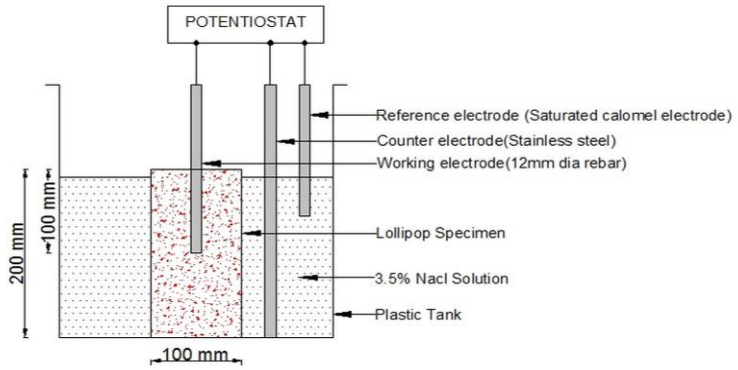

Figure 4. Schematic representation of polarization measurement setup.

3. RESULTS AND DESCRIPTION

3.1. Effect of paper sludge ash and curing condition on compressive strength

Table 4 displays the compressive strength values of GPC specimens that were acquired in accordance with Indian specifications.

Table 4. Compressive strength values of GPC.

Specimen ID	A0	B0	C0	A10	B10	C10
Compressive strength (N/mm^2)	53	32	17	40	39	38

Mechanical strength in the hardened geopolymer concrete serves as a key indicator of the effectiveness of the alternative source material because it gives a basic description of the caliber of the products of geopolymerization.For three curing conditions, the compressive strength of the concrete was assessed after 28 days. Under external exposure curing and ambient curing conditions, respectively, the FA-PSA-based geopolymer concrete's improvement in compressive strength was 21.88% and 123.53% higher than that of the non-PSA-based specimens.However, the addition of paper sludge ash under oven curingconditions had a negative impact on the strength performance of fly ash–based geopolymer concrete. The calcium compounds in the geopolymer mix increased the mechanical strength of the samples that were cured at room temperature due to paper sludge ash, but they decreased the strength of the samples that were cured at higher temperatures. When paper sludge ash containing calcium compounds was used, the pozzolanic reaction becomes more evident at low temperature than at elevated temperature, which may be due to the increase in the compressive strength of geopolymer concrete with paper sludge ash under ambient curingconditions. Fernández-Jimenez et al. [30] reported the same thing.In their study, they discovered that, in contrast to Ca compounds, Al and Si compounds were significantly more soluble at higher temperatures.This might be because of the existence of different hardening mechanisms [31].
But on day 28, it was found that the geopolymer concretewith paper sludge ash added had exceeded the desired strength of 35 MPa and had reached the significant strength of roughly 38 MPa for the 10% addition under external exposure curing and ambient curing conditions.

3.2. Effect of PSA and curing condition on the corrosion rate

Table 5 shows the LPR (ohms-cm^2), CR (mm/year), E_{corr} (mv)-free corrosion potential, and correspondingI_{corr} (μA/cm^2)-corrosion current density for the GPC concrete mixes 1 and 2 under three curing conditions, as obtained from the potentiostatic polarization data after the completion of exposure of geopolymer concrete to accelerate corrosion for about 20 days. Corrosion current density (I_{corr}) was seen as being proportional to CR.The specimen 100% fly ash–based geopolymer concrete mix had significantly lower I_{corr} (0.3×10^{-3} mA/cm^2) under oven curing condition in comparison to the other curing conditions. This could be because the fly ash–based geopolymer concretesamples, which undergo the curing process at high temperature of approximately 60°C, not only produce highest compressive strength [32, 33] but also had more positive potential values than the samples cured at low temperature [34]. It clarifies that the curing process makes the concrete to get denser and crystalline in structure. Under external exposure curing and ambient curing conditions, the fly ash based geopolymer concrete specimens showed higher I_{corr} values. This couldbe due to the low transition rate of the geopolymeric paste from liquid to solid, which takes place at low-temperature curing.

Table 5. Parameters obtained from corrosion analyzer through LPR and TP tests.

Parameters		**A0**	**B0**	**C0**	**A10**	**B10**	**C10**
LPR	Ohms-cm^2	27,722	2,041	1,153.8	3,060.85	5,454.5	11,726
CR	mm/year	0.348	4.825	8.305	3.685	1.63	0.832
E_{corr}	mV	253	515	535	419	395	398
I_{corr}	$\times 10^{-3}$ mA/cm^2	0.3	4.171	7.16275	3.18	1.41	0.718

The incorporation of 10% PSA into FA-GPC showed higherresistance to corrosion current as LPR for approximately 11726 ohm-cm^2 under AC condition compared to the two other curing conditions. Under OC condition, Mix 2 showed low resistance to current as LPR which was approximately 3060.85 ohm-cm^2. The precursor PSA in FA-PSA GPC contained calcium (Ca), which causedto the production of both the geopolymeric gel and the calcium aluminate silicate hydrate (CASH) gel at the same time. It resulted in filling up the gaps between the unreacted particles, and different hydrated phases resulted in formation of a homogeneous and dense matrix [35,36]. The geopolymeric gel and CASH gel are responsible for the pastes to have low ionic permeability [37]. Furthermore, adding calcium compound to samples that have been cured at room temperature speeds up the geopolymerization process, which is confirmed by data showing increased compressive strength and a correlation with lower porosity values. Insufficient three-dimensional geopolymeric aluminosilicate network growth under oven-cured samples causes increased porosity values [38], but calcium ions also contribute to silica and alumina ion dissolution from alkaline solution [39] and the development of compressive strength [40].

3.3. Destructive test on GPC samples

The pull-out tests were performed on the GPC lollipop specimens in a UTM after 20 days of accelerated corrosion exposure.The bond strength loss was determined and shown in Figure 5. The highest loss was shown by FA-GPC specimens under AC and EEC conditions. The loss was lowest for the OC-cured FA-GPC specimens, approximately 18%. In the FA-PSA GPC specimens, the bond strength loss was low under AC condition compared to that in the other two curing conditions.

3.4. Gravimetric weight loss measurement

The steel reinforcement bar was retrieved from the specimens after the pull-out test by breaking through it. The retrieved bar was cleaned of rust using chemicals as per the procedure mentioned by ASTM Standard G1-90 [29]. The actual mass loss of the steel-reinforcing bars was then calculated by weighing the bars. Figures 6 and 7 show the steel bars during and after rust removal. The mass loss percentages of the reinforced bar in FA-GPC and FA-PSA GPC specimens are shown in Figure 5. From the figure, it can be observed that the FA-GPC specimens show a higher mass loss percentage of

approximately 18.41% in the case of AC condition compared to the FA-GPC specimens under EEC and OC-cured conditions where the loss percentage is low.

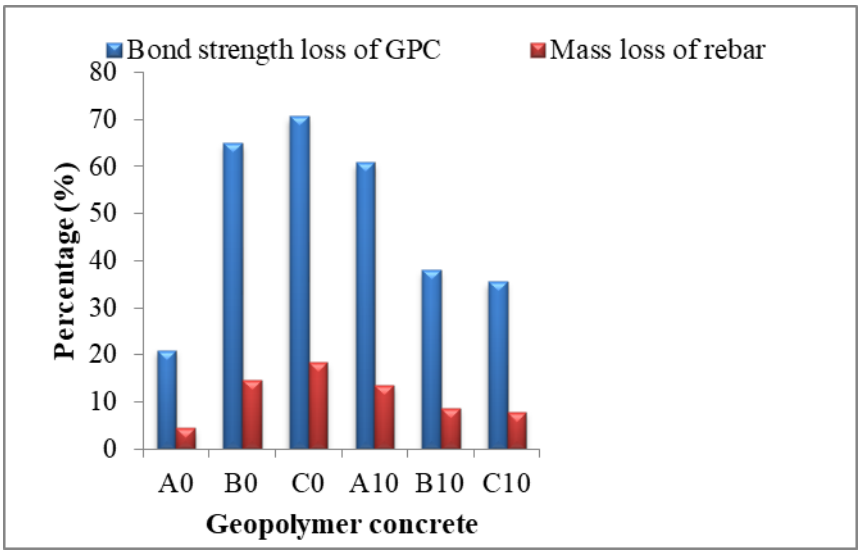

Figure 5. Bond strength and mass loss percentage of rebar in GPC.

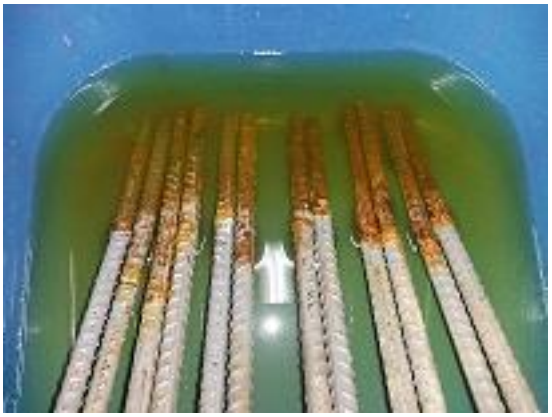

Figure 6. Steel rebar during rust removal as per ASTM Standard G1-90.

Figure 7. Steel rebar from GPC specimens after rust removal.

The inclusion of 10% PSA into FA-GPC under ambient curing and external exposure curing conditions effectively reduced the loss of mass by approximately 57% and 41%, respectively, compared to the FA-GPC under the same curing conditions. The percentage mass losses of the reinforcement bar in the GPC specimens of FA-GPC under oven curing, external exposure curing, and ambient curingconditions were 4.483%, 14.619%, and 18.41%, respectively, after accelerated corrosion testing. For FA-PSA GPC specimens, the losses were 13.645%, 8.67%, and 7.827%, respectively.

Owing to the presence of calcium in the source material of the burned PSA, FA-PSA GPC specimen's superior corrosion resistance under ambient curing and external exposure curing conditions compared to non-PSA GPC specimens under the same curing conditions may be explained by their compactness and homogenous structure[38].

It was discovered that, under the same curing conditions, the FA-PSA GPC samples had a larger mass loss % than non-PSA GPC samples under oven curing conditions. This accounts for the low steel concrete bond strength and high CR of the samples.

4. CONCLUSIONS

The following conclusions can be made based on the study results:

– FA-GPC specimens show better corrosion resistance under OC condition compared to the other curing conditions.

– FA-PSA GPC specimens show better corrosion resistance only under AC condition.

– Reinforced FA-GPC specimens exhibit high polarization resistance and low corrosion current density values under the OC condition compared to the other curing conditions.

– Corrosion potential and polarization resistance values of the FA-PSA GPC specimens are high under AC condition but lower than those of the FA-GPC under OC.

– In comparison to specimens under different curing conditions, the observed bond strength and mass loss percentage of the FA-GPC specimens under OC conditions were the highest and lowest, respectively.

– Also, the bond strength performance and mass loss percentage of the FA-PSA GPC specimen were better under AC condition compare to those under other curing conditions.

References

1. T. Armstrong, *International Cement Review*, Dorking(2017) Surrey, UK.
2. V.M. Malhotra, *Concr. Int.*, 21 (1999) 61.
3. K.K. Deevasan and R.V. Ranganath, *Construct. Mater*., 164 (2011) 43.
4. A. Palomo, M.W. Grutzeck and M.T. Blanco, *Cem. Concr. Res.*,29 (1999) 1323.
5. D.V. Reddy, J.B. Edouard, K. Sohban and S.S. Rajpathak, Durability of Reinforced Fly Ash based Geopolymer Concrete in the Marine Environment, Proceedings of 36th Conference on Our World in Concrete and Structures, Singapore,2011.
6. M. Babaee and A. Castel,*Cem. Concr. Res.*, 88 (2016) 96.
7. D.M. Bastidas, A. Fernández-Jiménez, A. Palomo and J.A. González, *Corr. Sci.*, 50 (2008) 1058.

8. F.U.A. Shaikh,*Adv. Concr. Constr.*, 2 (2014) 109.
9. K.K. Patil and E.N. Allouche, *J. Mater. Civil Eng*., 25 (2012) 1465.
10. M. Olivia and H.R. Nikraz, Incorporating Sustainable Practice in Mechanics of Structures and Materials, CRC Press, Melbourne (2011) Victoria, Australia, 781–786.
11. A.M. Aguirre-Guerrero, R.A. Robayo-Salazar and R.M. de Gutierrez, *Appl. Clay Sci.*,135 (2017) 437.
12. W.M. Kriven, M. Gordon, B.L. Ervin, and H. Reis, *Ceram. Eng. Sci. Proc.*,28 (2009) 373.
13. C. Tennakoon, A. Shayan, J.G. Sanjayan and A. Xu, *Mater. Design*, 116 (2017) 287.
14. S. Astutiningsih, A. Rustandi and D. Noermala Sari, *Civil Eng. Dimen.*, 15 (2013) 89.
15. S. Yananand and K. Sagoe-Crentsil, *J. Environ. Manag.*, 112 (2012) 27.
16. R. García, R. Vigil de la Villa, I. Vegas, M. Frías and M.I. Sánchez de Rojas,*Constr. Build. Mater.*, 22 (2008) 1484.
17. R.M. Ridzuan, A.A. Khairulniza, M.A. Fadzil, J. Nurlizaand and M.A.M. Fauzi, Alkaline Activators Concentration Effect to Strength of Waste Paper Sludge Ash-based Geopolymer Mortar, Proceedings of the International Civil and Infrastructure Engineering Conference, Singapore, 2013, 169–175.
18. S. Bernal, R. Ball, O. Hussein and A. Heath, *J. Provis*, Paper Sludge Ash as a Precursor for Production of Alkali-Activated Materials, Second International Conference on Advance Chemically Activated Materials, Eddie, Changsha, China, 2014,140–149.
19. A. Battaglia, N. Calace, E. Nardi, B. M. Maria Petronio and M. Pietroletti, *Microchem. J.*,75 (2003) 97.
20. X. Geng, J. Dengand S.Y. Zhang, *J. Wood Fiber Sci*., 38 (2006) 736.
21. J. Bai, A. Chaipanich, J.M. Kinuthia, M. O'Farrell, B.B. Sabir, S. Wild and M.H. Lewis, *Cem. Concr. Res.*, 33 (2003) 1189.
22. M. Frías, O. Rodríguez, I. Vegas and R. Vigil, *J. Am. Ceram. Soc.*, 91 (2008) 1226.
23. S.P. Mun and B.J. Ahn, *J. Indus. Eng. Chem.*, 7 (2001) 292.
24. Nordtest Method NT Build 356: Concrete, Repairing Materials and Protective Coating: Embedded Steel Method, Chloride Permeability, Espoo, Finland, 1989.
25. R.P. Brown and R.J.Kessler, An Accelerated Laboratory Method for Corrosion Testing of Reinforced Concrete Using Impressed Current, Florida Department of Transportation Research,RIMLNo.206 October, 1978.
26. M. Sahmaran, V.C. Li and C. Andrade, *ACI Mater. J.*,105 (2008) 243.
27. M. Stern and A.L. Geary, *J. Electrochem. Soc*., 104 (1957) 56.
28. ASTM G59, *Standard Test Method for Conducting Potentiodynamic Polarization Resistance Measurements*, American Society for Testing and Materials, Philadelphia, PA, USA, 2003.
29. ASTM G1, *Standard Practice for Preparing, Cleaning, and Evaluating Corrosion Test Specimens*, American Society for Testing and Materials, Philadelphia, PA, USA, 2000.
30. A. Fernández-Jimenez, I. García-Lodeiroand A. Palomo, Development of New Cementitious Materials by Alkaline Activating Industrial By-Products, Second International Conference on Innovative Materials, Structures and Technologies, IOP Conference Series: Materials Science and Engineering 96-012005 Ed.Anete Ashton, Riga, Latvia, 2015.
31. C. Shi, P.V. Krivenko and D. Roy, *Alkali-Activated Cements and Concrete*, Taylor and Francis (2006) Oxford, London and New York.
32. B.V. Rangan, Low-Calcium Fly-Ash-Based Geopolymer Concrete, Faculty of Engineering, Curtin University of Technology, Perth, Australia, 2008, 1–19.
33. J.C. Swanepoel and C.A. Strydom, *Appl. Geochem.*, 17 (2002) 1143.
34. Z.F. Farhana, H. Kamarudin, A. Rahmat, and A.M. Mustafa Al Bakri, *Austr. J. Basic Appl. Sci.*, 7 (2013) 230.
35. S. Puligilla and P. Mondal, *Cem. Concr. Res.*, 43 (2013) 70.
36. Y. Luna-Galianoa, C. Fernández-Pereiraa and M. Izquierdob,*Mater. Constr.*, 324 (2016) 66.

37. R.L. Redmond, J.L. Provis and J.S. J. van Deventer, *Cem. Concr. Res.*, 40 (2010) 1386.
38. H. Khater, *J. Mater. Civil Eng.*, 24 (2012) 92.
39. K. Srinivasan and A. Sivakumar, *Constr. Mater.*, 168 (2015) 24.
40. X. Guo, H. Shi, *Adv. Cem. Res.*, 27 (2015) 559.